1/1

PREPRINT UCRL- 79777

CONF-771136--29

Lawrence Livermore Laboratory

A MINIATURE X-RAY POINT SOURCE FOR ALIGNMENT AND CALIBRATION OF X-RAY OPTICS

Robert H. Price, Michael J. Boyle and S. S. Glaros

MASTER

November 1, 1977

This paper was prepared for submission to the APS Plasma Physics Meeting of the American Physical Society, Atlanta, Georgia, November 5-11, 1977.

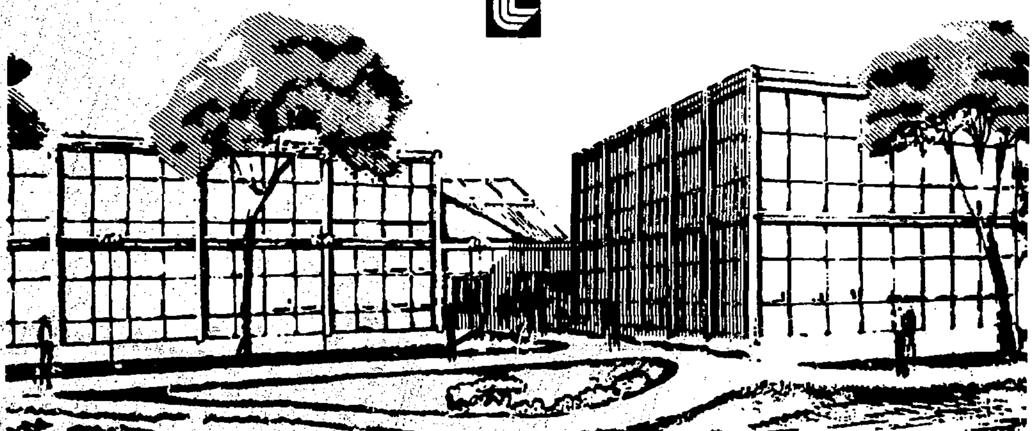

Abstract Submitted

for the APS Plasma Physics Meeting of the

American Physical Society

November 5-11, 1977

Physics and Astronomy
Classification Scheme
Number 52

Bulletin Subject Heading in
which Paper should be placed
Plasma Diagnostics

A Minature X-Ray Point Source for Alignment and Calibration of X-Ray Optics. Robert H. Price, Michael J. Boyle and S. S. Glaros, Lawrence Livermore Laboratory.**--A minature x-ray point source of high brightness similar to that of Rovinsky, et al.[1] is described. One version of the x-ray source is used to align the x-ray optics on the Argus and Shiva laser systems. A second version is used to determine the spatial and spectral transmission functions of the x-ray optics. The spatial and spectral characteristics of the x-ray emission from the x-ray point source are described. The physical constraints including size, intensity and thermal limitations, and useful lifetime are discussed. The alignment and calibration techniques for various x-ray optics and detector combinations are described.

**Supported by U. S. ERDA Contract W-7405-ENG-48

1 B. M. Rovinsky, V. G. Lutsau and A. I. Avdeyenko, in V. E. Cosslett et al., *X-Ray Microscopy and Microradiography*, Academic Press, Inc., New York, 1957, pp. 269-277.

Submitted by

Robert H. Price
University of California
Lawrence Livermore Laboratory
P. O. Box 808, L-549
Livermore, CA 94550

A MINIATURE X-RAY POINT SOURCE FOR ALIGNMENT AND CALIBRATION OF X-RAY OPTICS

Robert H. Price, Michael J. Boyle and S. S. Glaros

This report is a brief preliminary summary of a more extensive report detailing work carried out on the development of a miniature point x-ray source, similar to that of Rovinsky, et al,[1] for the alignment and calibration of the x-ray optics planned for the Argus and Shiva laser systems. X-ray microscopes of both the Wolter hyperboloid-ellipsoid axisymmetric type[2] and the four-channel Kirkpatric-Baez type[3] are mounted on the target chamber as shown in Fig. 1. The axisymmetric microscopes are capable of submicron resolution over a field of view of several hundred microns as shown in Fig. 2. The four-channel Kirkpatrick-Baez microscopes should also be capable of submicron resolution.

For alignment purposes, the "side on" version of the miniature point x-ray source is placed in the target position. Polaroid photos of the x-ray source are then taken through the x-ray microscope as adjustments are made to point and focus the x-ray microscope. The smallest dimension of the x-ray emitting region is approximately 1 μm so that resolution measurements can be made as the alignment proceeds.

A second version of the point x-ray source is used for spatial and spectral calibration of the x-ray optics. Various aspects of this work are discussed briefly in subsequent sections of this paper.

The "Side on" Version of the Point X-ray Source

The "Side On" point x-ray source (Fig. 3) is used for alignment of the x-ray optics planned for the Argus and Shiva laser systems. Design criteria for this device include: high brightness, small x-ray emission region, visibility from many directions, operating vacuum of 10^{-4} torr, simplicity of operation, and a unit size and weight consistent with mounting on the target positioner. The tungsten needle anode of the x-ray source is operated at 16 kV and draws 1 to 5 μa. The electron current arrives at the needle tip from the small tungsten loop filament after passing through a small limiting aperture.

Figure 4 is an image of the x-ray emission region magnified 45 times. Figure 5 is magnified 136 times. The x-ray flux from both versions of the point x-ray source is approximately 10^{10} photons/sec into 4π steradians.

The "End on" Version of the Point X-Ray Source

This version of the point x-ray source (Fig. 6) is used for spatial and spectral calibration of the x-ray microscopes planned for the Argus and Shiva laser systems. The device consists of (Fig. 7): 1) a tungsten needle anode at 16 kV with a point radius of typically less than 1000 Å; 2) a hemispherical cavity centered around the needle tip which shapes the electric field lines; 3) an aperture through which electrons are allowed to pass towards the needle tip; and 4) a tungsten loop filament which emits the electrons that bombard the tungsten anode. The anode current is typically in the range of 1 to 3 μa. The x-ray emission is viewed along the needle axis through the focusing aperture and the surrounding filament loop. The emission region imaged through a 9x axisymmetric x-ray microscope is shown in Fig. 8. The spot is 25 μm FWHM, of which 15 μm is attributed to the x-ray source, 5 μm to the resolution of the microscope, and 5 μm to imperfect focusing.

Production of Tungsten Needles for the Point X-Ray Source

The tungsten needles used in the point x-ray source are electrolytically etched in 1N NaOH using a low voltage 1 KHz alternating current. Hydrogen evolves during one half cycle and etching takes place during the other half cycle. The convection currents from the bubbling hydrogen gas locally affect the etching rate and produce the characteristic shape of the needle tip. As the etching proceeds, the surface area of the needle tip is reduced, causing the etching current to drop. A circuit senses the etching current and as it falls below a preset threshold, turns off the etching current and indicates that the needle is finished. The parameters which affect the needle tip shape are: the etching voltage and current; the initial diameter of the wire; the distance the wire is immersed in the etchant; and the threshold for etching current cutoff. The needles made in this way are very reproducible. An optical micrograph of a typical needle is shown in Figure 9. Scanning electron micrographs of the tip of the needle are shown in Figure 10.

Needles can be made of materials other than tungsten, however, there will be some reduction in the power dissipation of the needle tip in the x-ray source due to the lower melting point of other materials.

Lifetime and Power Dissipation of the Needle Tip

While in operation, there is an intense power flux incident upon the needle which will tend to degrade its point. Evaporation of the needle tip will occur at a rate dictated by its temperature. Figure 11 is a plot of the time for the needle to evaporate back 1 μm, versus temperature at the tip. With a cone angle of order 10°, a loss of 1 μm of tip length would produce an insignificant increase in spot size. As seen from the plot, evaporation from the tip is insignificant for temperatures in the neighborhood of 2400-2500°K.

It is readily shown that power dissipation (P) at the tip scales as:

$$\frac{P}{R \tan \Theta} = C_0 \, (T_0, T_1)$$

where Θ is the needle tip half angle, R is the radius of the x-ray emission region observed looking toward the needle tip along its axis, and C_0 (T_0, T_1) is a simple function of the tip temperature (T_0) and the temperature of the ultimate heat sink (T_1). C_0 (T_0, T_1) is plotted in Figure 12 for two values to T_1.

A needle operated for several days at 16 kV and currents of 1 to 5 μa is shown in Figure 13.

The tip is also potentially subject to distortion due to the $\frac{E^2}{8\pi}$ pressure of the electric field, approximately $3 \times 10^9 \frac{\text{dynes}}{\text{cm}^2}$; however, to date no such distortion has been observed.

Spectral Measurements with the Point X-Ray Source

Although needles of materials other than tungsten may be used to generate characteristic line radiation, the point x-ray source is designed primarily to produce bremsstrahlung. A spectrum of the x-ray emission from the point x-ray source seen through a pinhole is shown in Figure 14. At energies less than 1.5 keV the flux was attenuated by the 0.001-inch Be window of the lithium drifted silicon detector. The tungsten M lines at 1.8 keV and the tungsten Lα lines at 8.4 keV are clearly visible. Figure 15 is a spectrum of the point source seen through a 9x axisymmetric microscope with 1° grazing incidence nickel mirrors. The quotient of the two spectra yields an absolute measurement of the effective solid angle of the x-ray mirror as a function of energy. This calibration curve is shown in Figure 16.

Acknowledgements

The authors would like to thank H. Ahlstrom and E. Storm for their support and encouragement during this work. Others in Y-Division to whom thanks should be given are R. Dunham, K. Andrus, and T. Schwinn for their mechanical support; D. Campbell, E. Powell and J. Stewart for electronics support; and D. Hughes and D. Holeman for general support. Thanks also go to G. Burginyon, J. Gaines, E. Augusta, R. Crab, L. Paxton, D. Brown and others in L-Division of LLL, who assisted in the early part of this work.

References

1. B. M. Rovinsky, V. G. Lutsau, and A. I. Avdeyenko, in V. E. Gosslett, at al, X-Ray Microscopy and Microradiography, Academic Press, Inc., New York, 1957, pp. 269-277.

2. Wolter, H., "Mirror Systems with Grazing Incidence Mirrors as Image-Forming Optics for X-Rays", Ann. Physik, Vol. 10, 94, 1952.

3. P. Kirkpatrick and A. V. Baez, "Formation of Optical Images with X-Rays", J. Opt. Soc. Amer., 38, 766, 1948.

Fig. 1

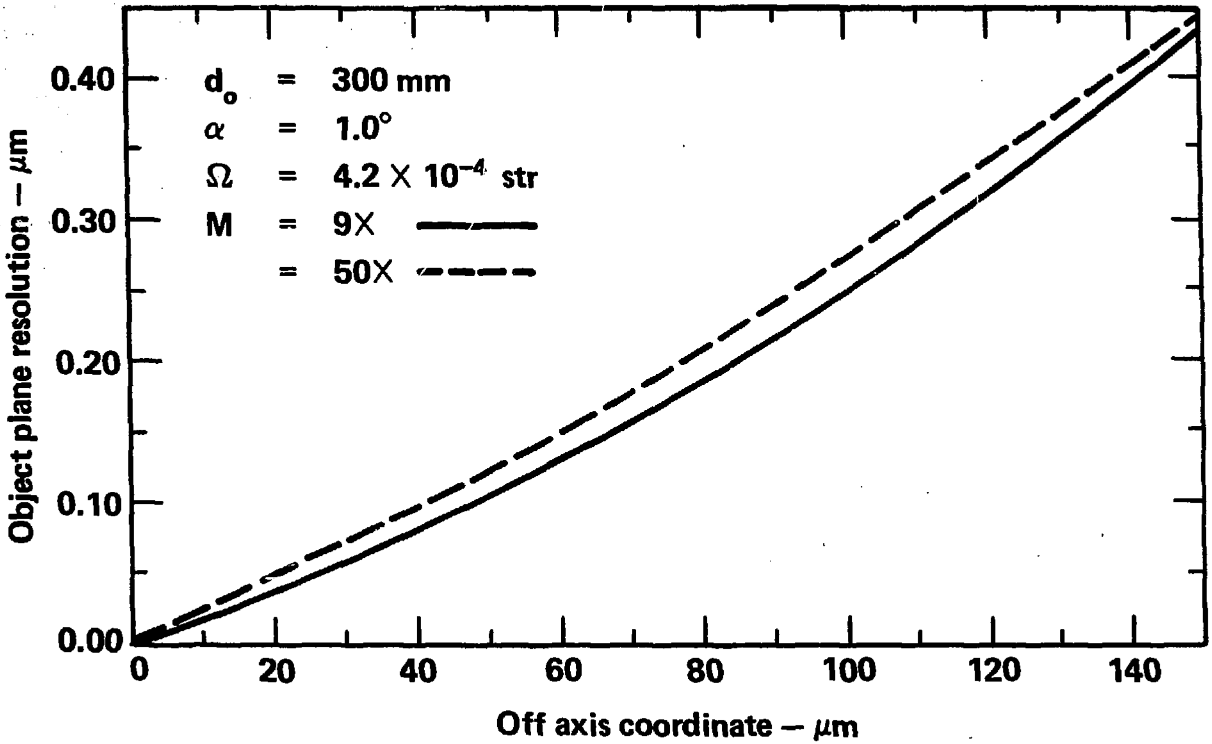

Object plane resolution – μm
0.40
0.30
0.20
0.10
0.00
d₀ = 300 mm
α = 1.0°
Ω = 4.2 X 10⁻⁴ str
M = 9X
= 50X
0
20
40
60
80
100
120
140
Off axis coordinate – μm

Fig. 2

Fig. 3

Fig. 4

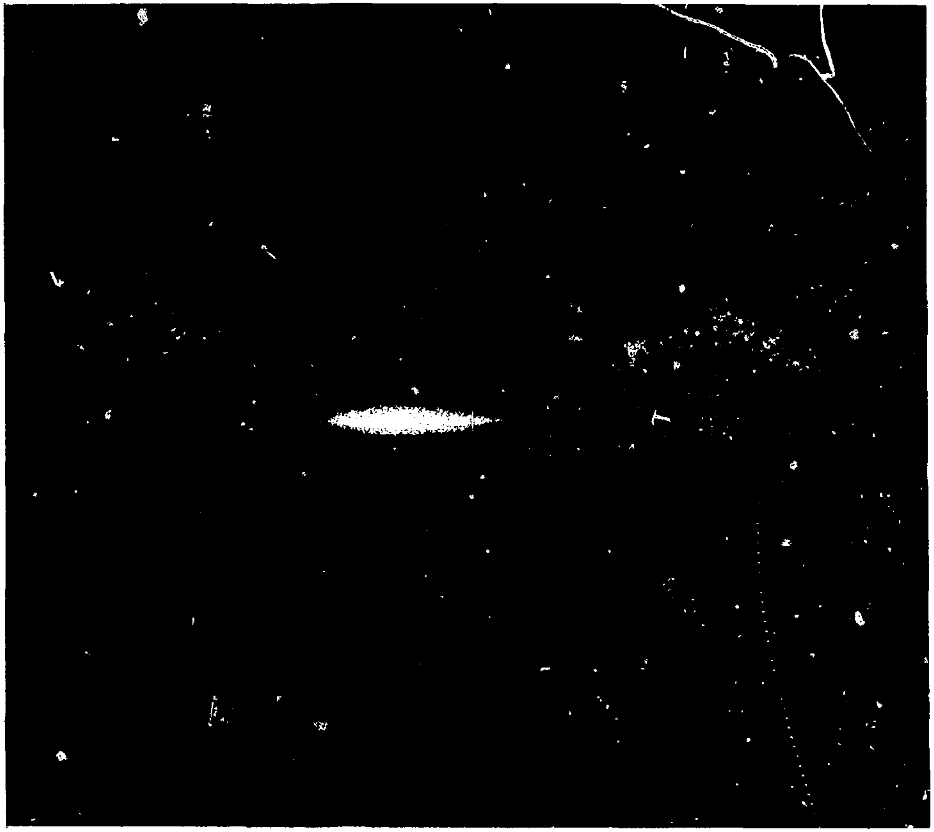

100 µm

Fig. 5

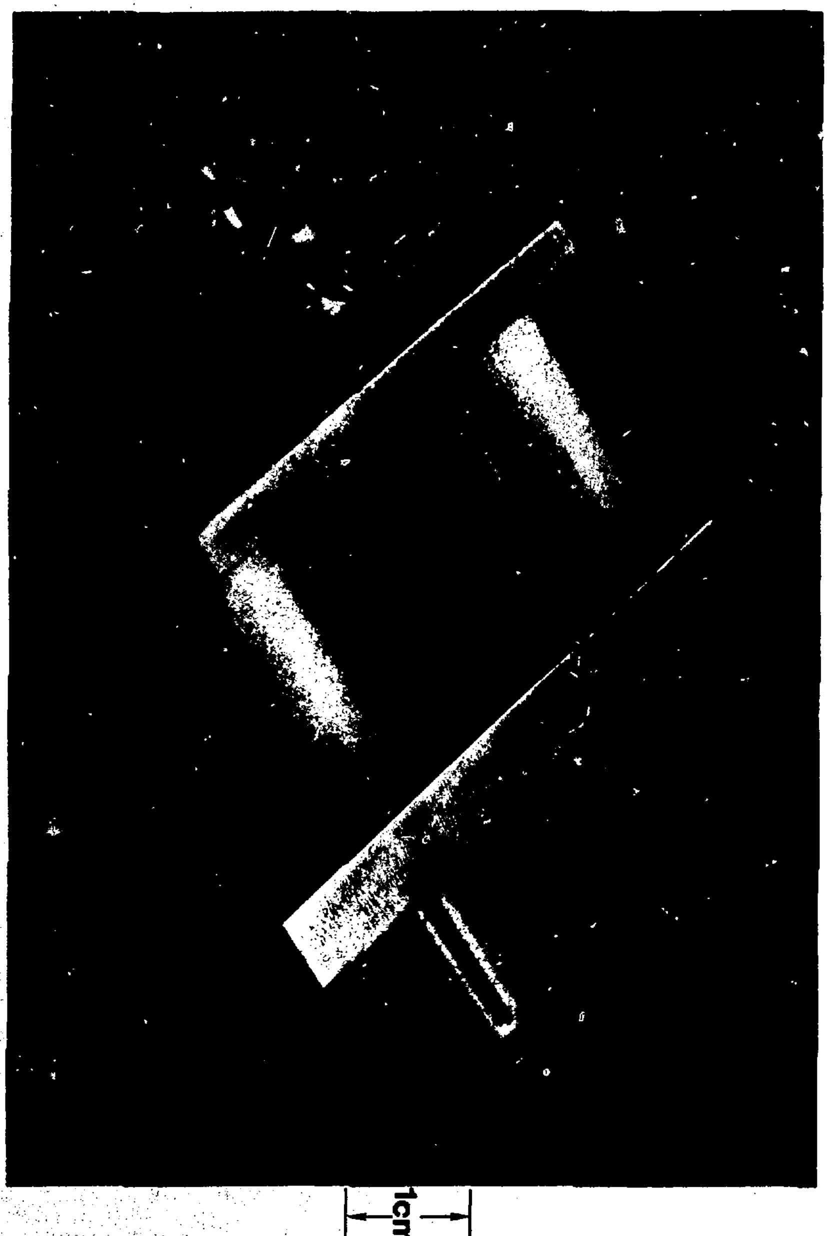

Fig. 6

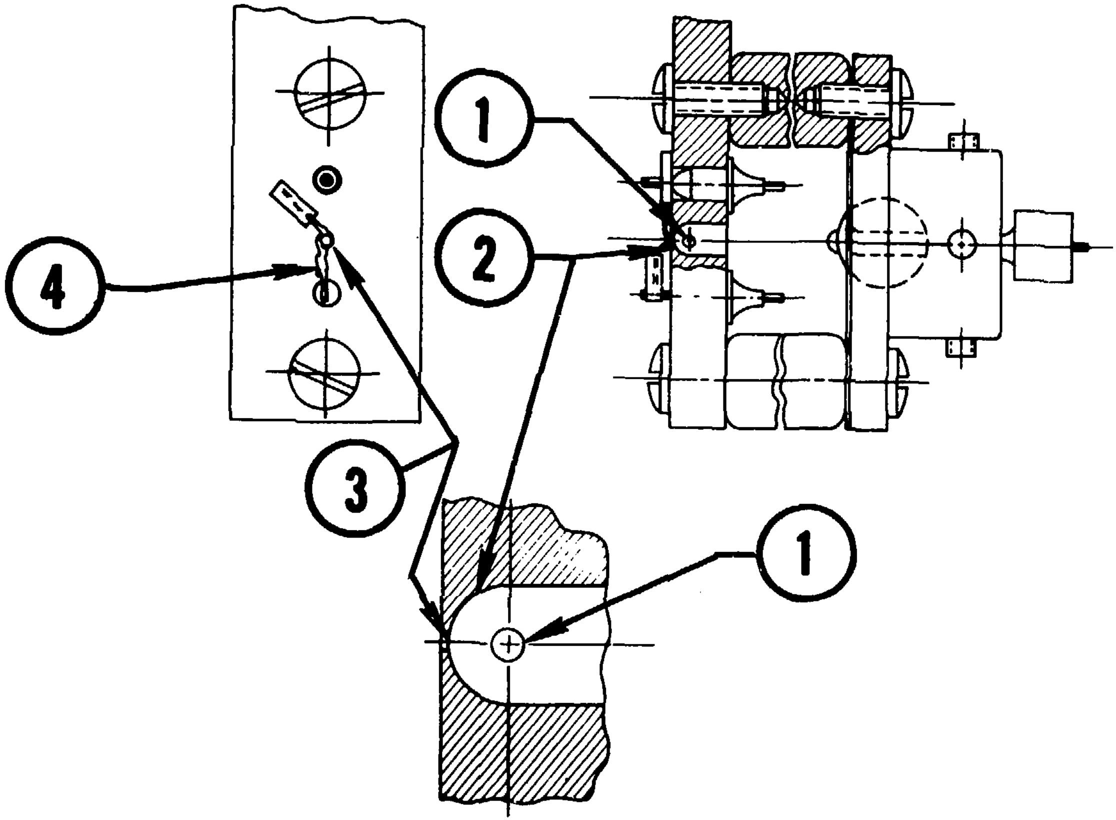

Fig. 7

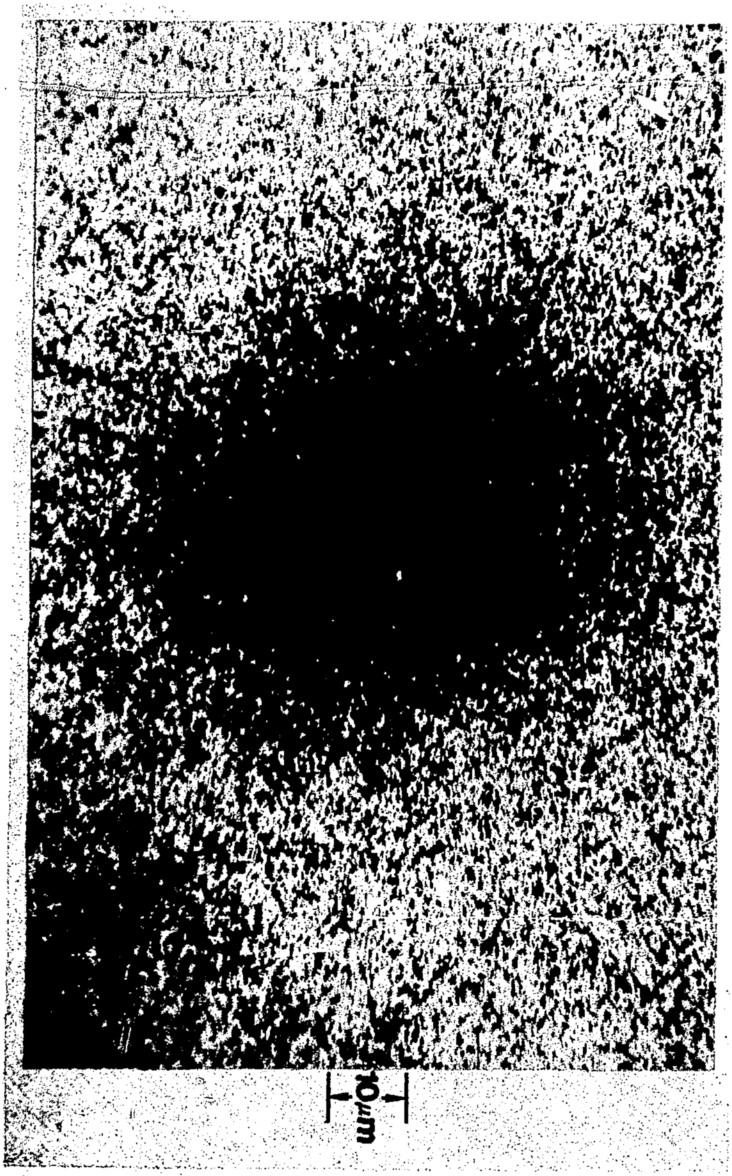

Fig. 8

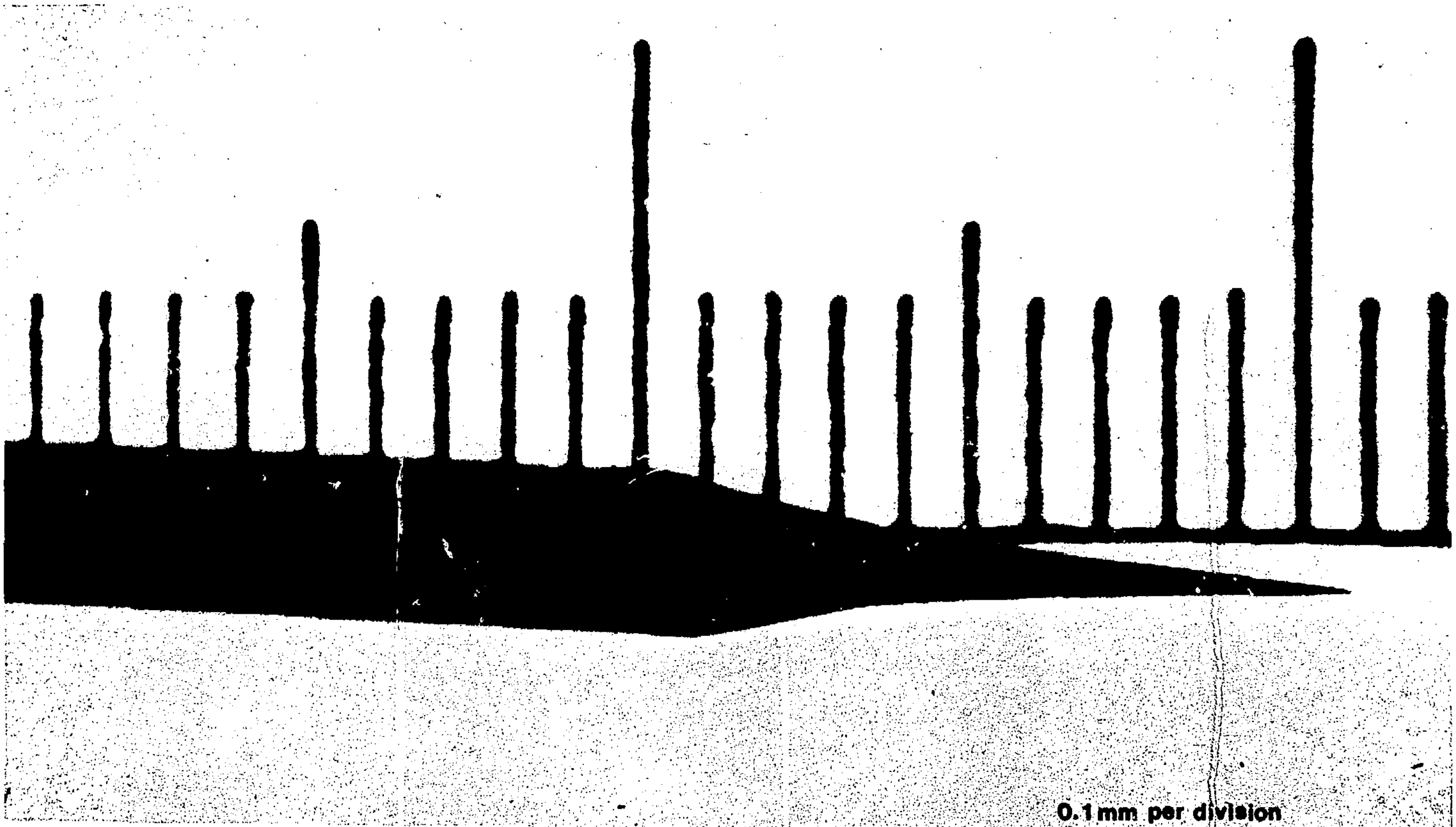

Fig. 9

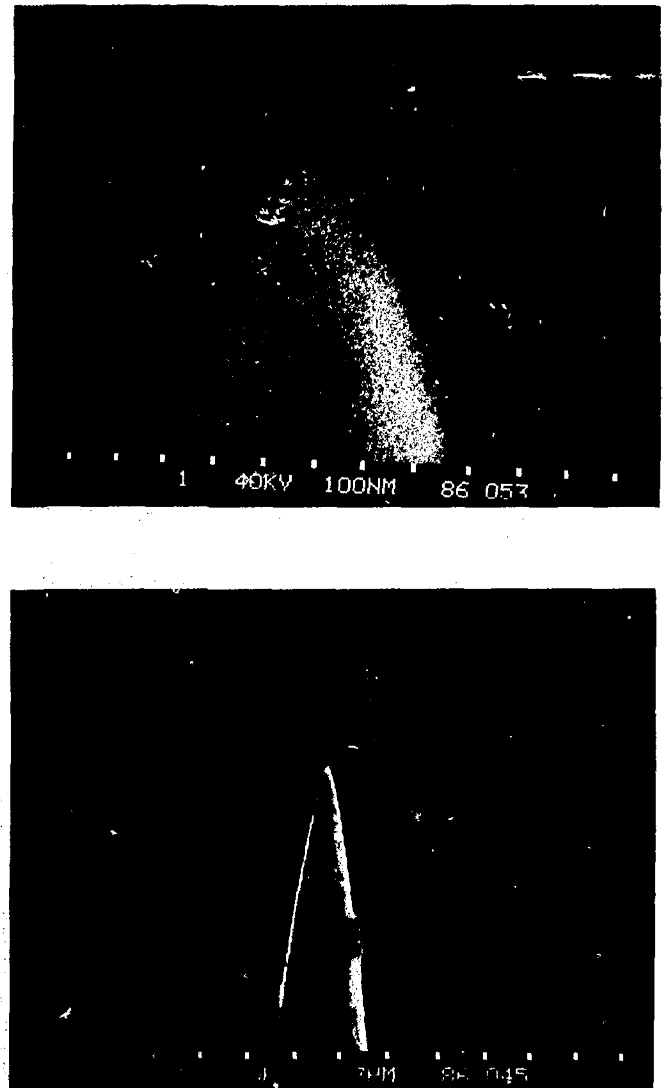

Fig.10

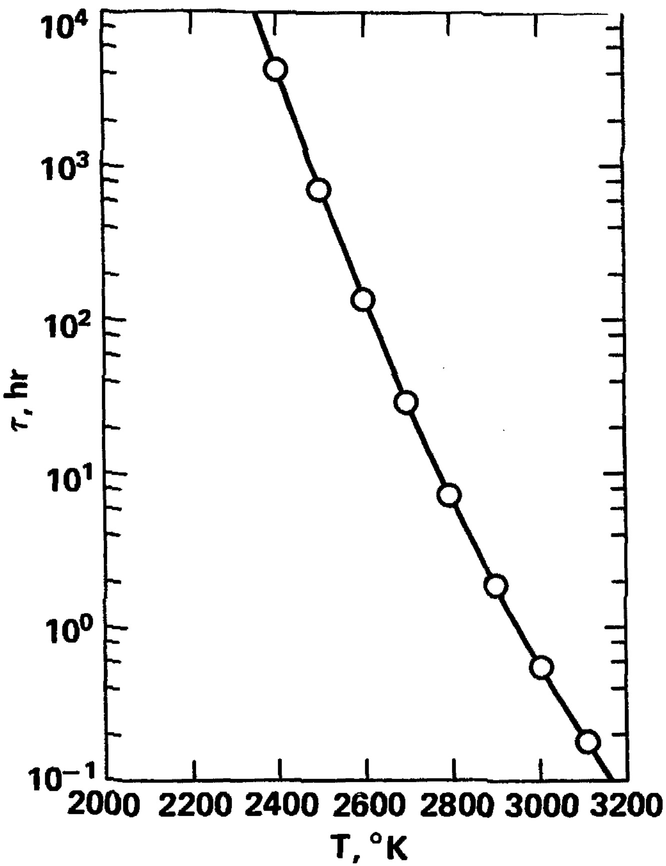

10^4
10^3
10^2
10^1
10^0
10^{-1}
τ, hr
2000 2200 2400 2600 2800 3000 3200
T, °K

Fig. 11

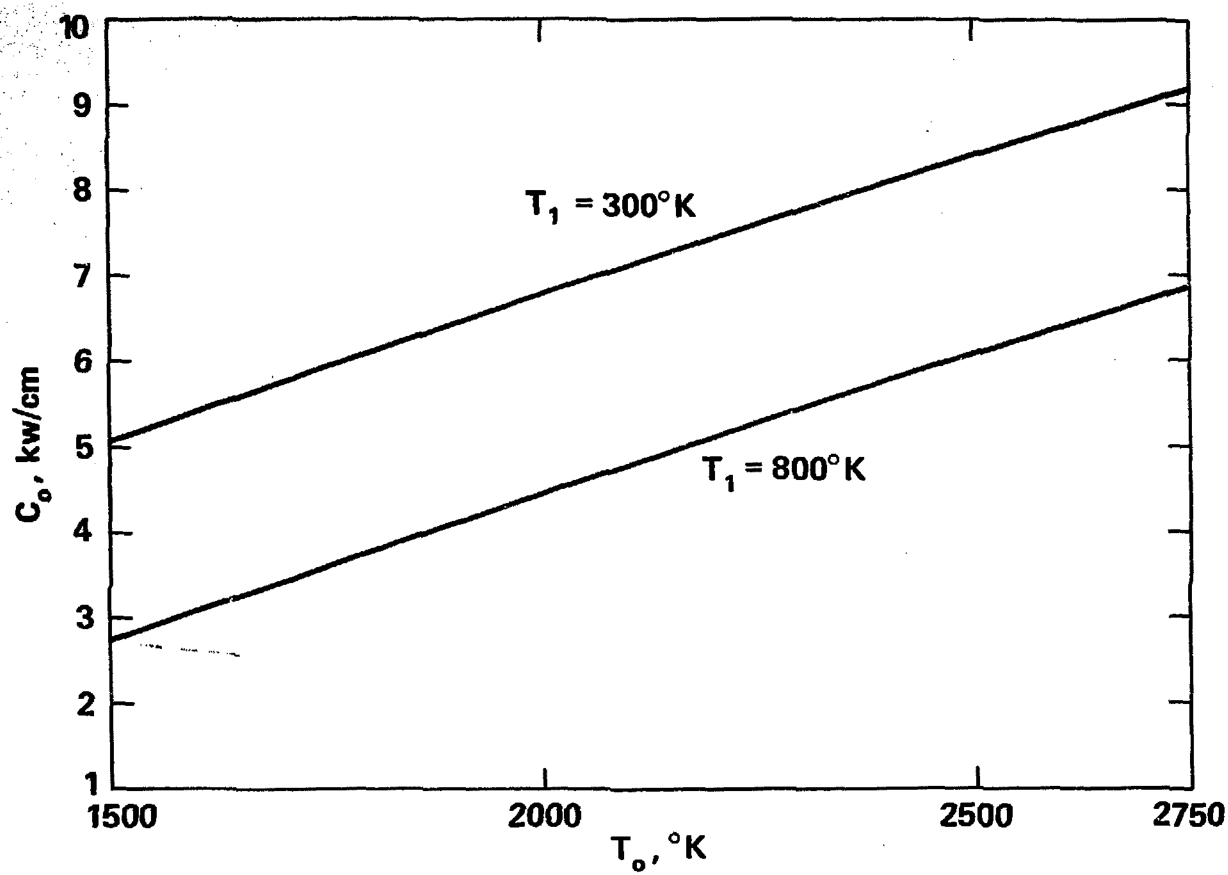

Fig. 12

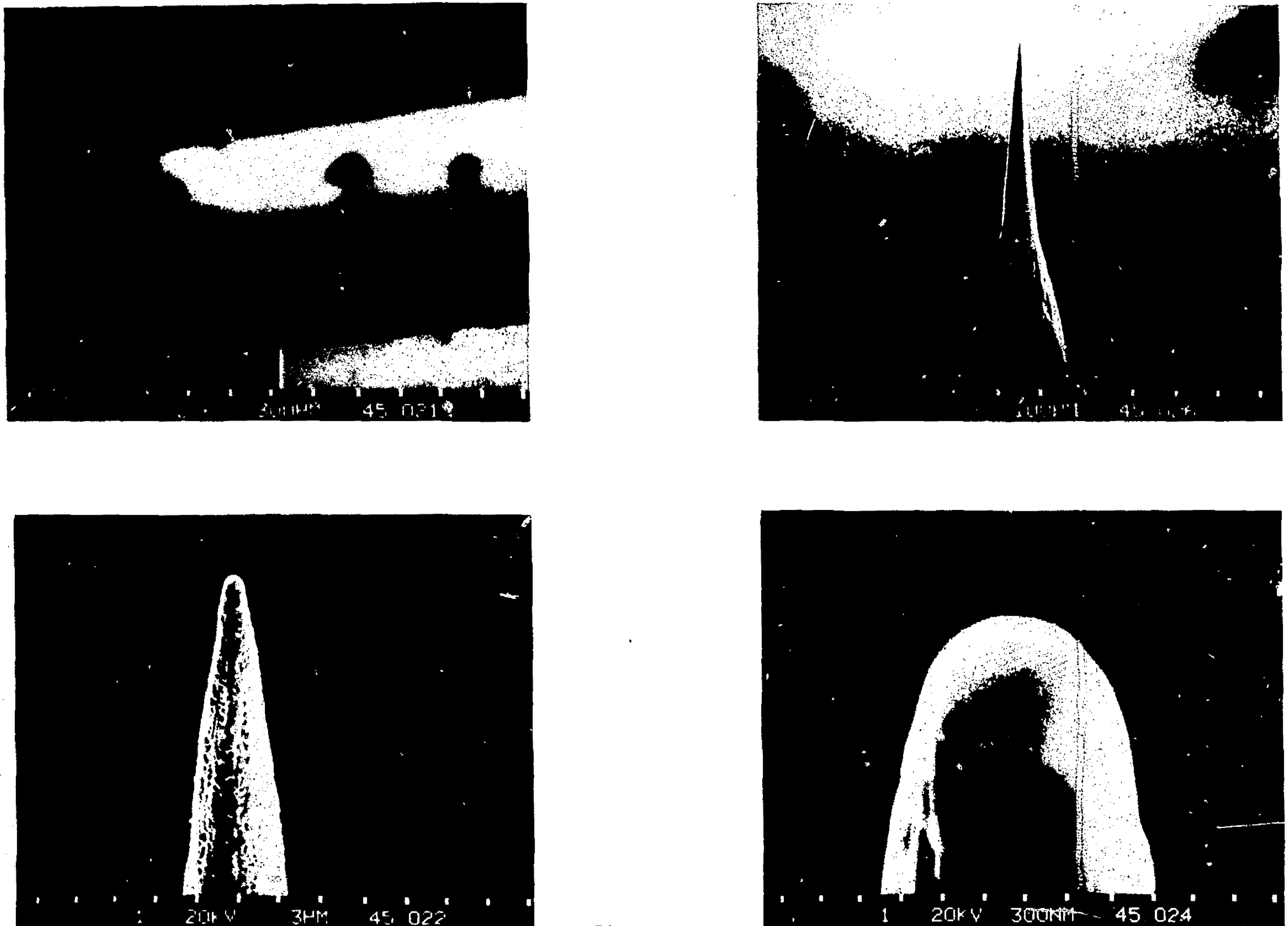

Fig. 13

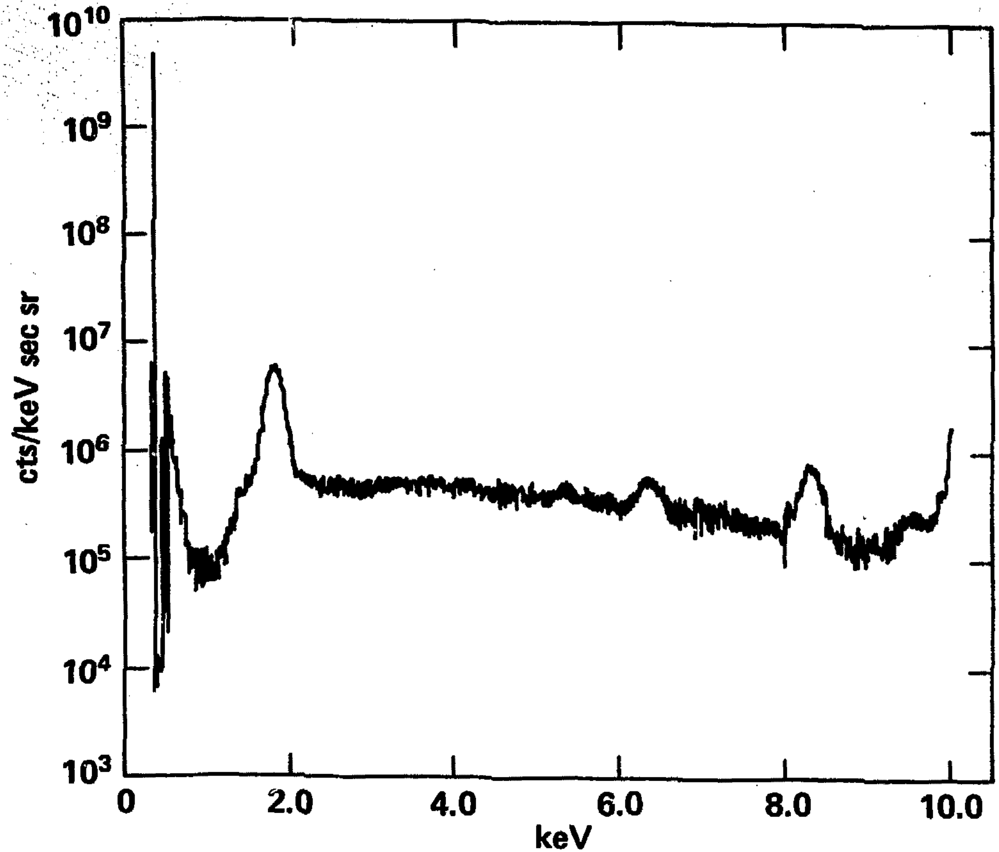

10^10
10^9
10^8
10^7
10^6
10^5
10^4
10^3
cts/keV sec sr
0
2.0
4.0
6.0
8.0
10.0
keV

Fig. 14

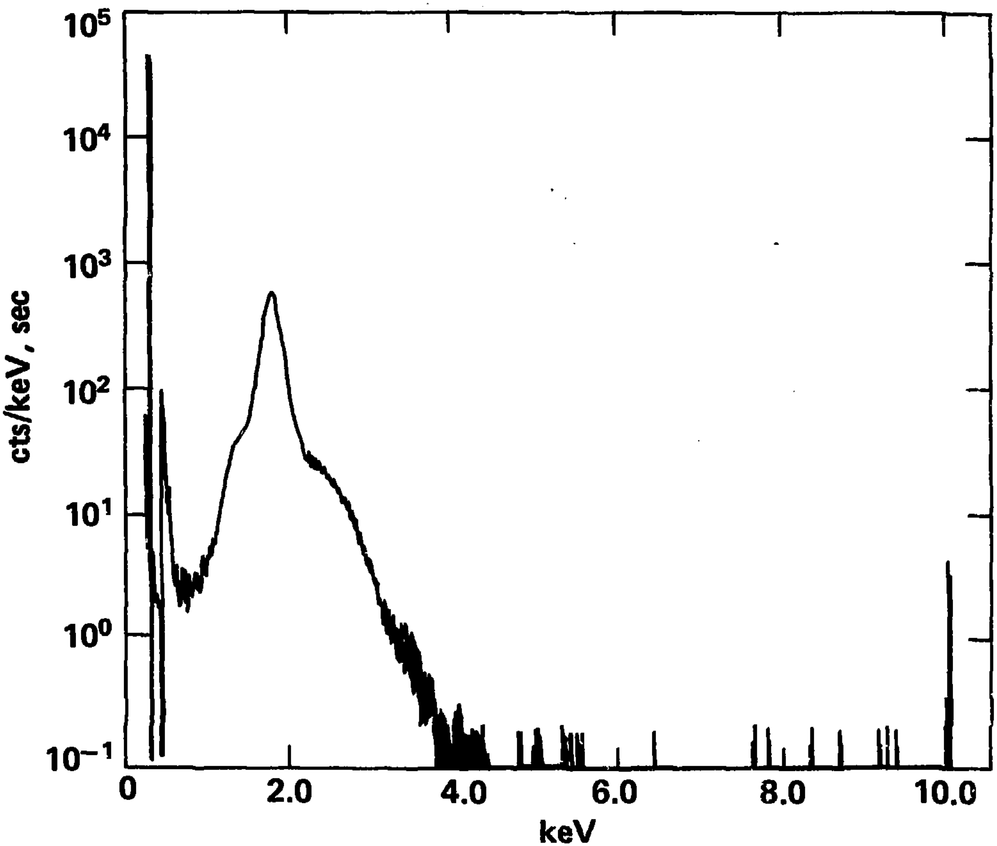

Fig. 15

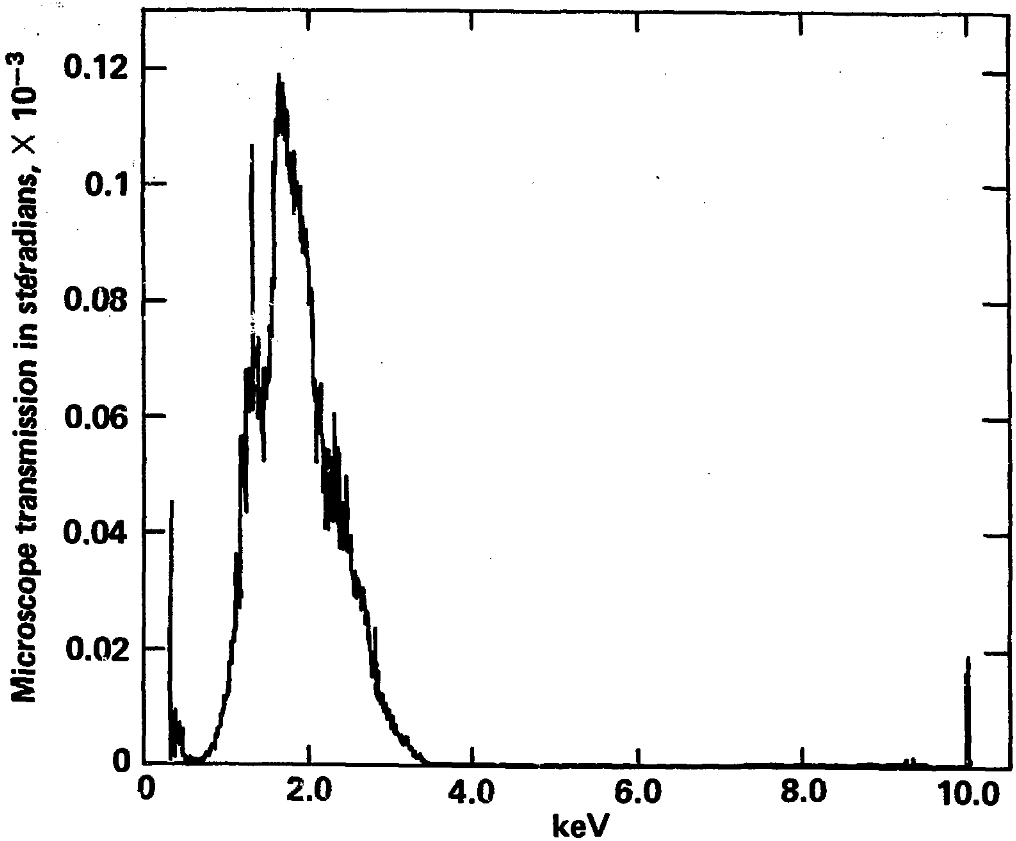
Microscope transmission in stéradians, × 10−3
0.12
0.1
0.08
0.06
0.04
0.02
0
0
2.0
4.0
6.0
8.0
10.0
keV

Fig. 16